A 3D MULTI-PLATE ENVIRONMENT FOR SOUND SYNTHESIS

*Alberto Torin**
Acoustics and Audio Group
University of Edinburgh
Edinburgh, UK
A.Torin@sms.ed.ac.uk

Stefan Bilbao
Acoustics and Audio Group
University of Edinburgh
Edinburgh, UK
sbilbao@staffmail.ed.ac.uk

ABSTRACT

In this paper, a physics-based sound synthesis environment is presented which is composed of several plates, under nonlinear conditions, coupled with the surrounding acoustic field. Equations governing the behaviour of the system are implemented numerically using finite difference time domain methods. The number of plates, their position relative to a 3D computational enclosure and their physical properties can all be specified by the user; simple control parameters allow the musician/composer to play the virtual instrument. Spatialised sound outputs may be sampled from the simulated acoustic field using several channels simultaneously.

Implementation details and control strategies for this instrument will be discussed; simulations results and sound examples will be presented.

1. INTRODUCTION

Non-linear vibrations of thin plates have been the object of intense study [1]. Typical phenomena, like crashes and pitch glide effects, cannot be captured by a linear model, and these constitute, probably, some of the most interesting features of these objects from a perceptual perspective. The use of these elements in a sound synthesis environment becomes, therefore, a very attractive possibility. Amongst the first attempts at simulating gongs sounds we can cite the work of Van Duyne *et al.* (see, e.g., [2] for a complete summary.) More recently, sound synthesis of non-linear plates using a modal approach has been performed by Ducceschi *et al.* with convincing results [3].

When it comes to sound synthesis of percussion instruments, modularity seems to be the key word, from the well-known CORDIS-ANIMA [4] and Mosaic/Modalys systems [5, 6], to more recent works by Bilbao [7] and Avanzini *et al.* [8]. Several basic elements can be combined at the user's discretion in order to create a complex system that can serve as a virtual instrument. Following this approach, in this paper we present a sound synthesis environment composed of several non-linear thin plates. The main novelty of this work is the introduction of an explicit coupling between the plates and the surrounding air.

The underlying physical model of this system will be described in Section 2, while a numerical implementation based on finite difference time domain methods will be discussed in Section 3. In Section 4, a brief outline of instrument design and control issues will be presented. Finally, simulation results and sound examples can be found in Section 5.

* This work was supported by the European Research Council, under grant StG-2011-279068-NESS.

2. DESCRIPTION OF THE MODEL

The system under analysis is composed of several plates housed in a 3D enclosure $\mathcal{V}$ of air, with which they are coupled (see Figure 1.) Simulations of instruments embedded in 3D have already been performed in the past [9, 10], and this work adopts the same approach.

2.1. Plates

The main components of this model are N thin plates defined over rectangular regions $\mathcal{P}_i$ with $i = 1, \ldots, N$, all parallel to the xy plane, and with centres at coordinates $\mathbf{x}_c^{(i)} = (x_c^{(i)}, y_c^{(i)}, z_c^{(i)})$. As usual, the main physical variable is the transverse displacement $w(x, y, t)$ of the plate, at position (x, y) and time t. The equations of motion for the i-th plate are those for stiff objects with viscoelastic loss [11] and geometric non-linearities [12] (generally referred to as von Kármán equations, in the literature), and can be written as:

$$\partial_{tt} w^{(i)} = -\kappa_i^2 \Delta_{2D}^2 w^{(i)} + \sigma_i \Delta_{2D} \partial_t w^{(i)} + \frac{1}{\rho_i H_i} \mathcal{L}(w^{(i)}, \Phi^{(i)}) + \frac{1}{\rho_i H_i}(f_i^+ + f_i^-) + \frac{1}{\rho_i H_i} \delta(x_i - x_{exc}, y_i - y_{exc}) f_{i,exc}. \tag{1}$$

The differential operators Δ_{2D} and Δ_{2D}^2 are the Laplacian and biharmonic operators, respectively, with $\Delta_{2D} = \partial_{xx} + \partial_{yy}$. The stiffness parameter κ_i is defined as:

$$\kappa_i = \sqrt{E_i H_i^2 / 12 \rho_i (1 - \nu_i^2)}, \tag{2}$$

where (dropping the subscripts) ρ is the plate density, in kg/m^3, H is the thickness, in m, E is Young's modulus, in kg/s^{2}m, and ν is the dimensionless Poisson's ratio. σ is the coefficient governing viscoelastic losses, in m^2/s. All these parameters can in principle be distinct for the various plates.

The last term in the first line of (1) is responsible for non-linear effects and can be obtained from a fuller model when in-plane inertia is neglected [12]. When acting on two test functions ξ and χ, the operator $\mathcal{L}$ gives:

$$\mathcal{L}(\xi, \chi) = \partial_{xx}\xi \partial_{yy}\chi + \partial_{yy}\xi \partial_{xx}\chi - 2\partial_{xy}\xi \partial_{xy}\chi. \tag{3}$$

$\Phi(x, y, t)$ is the so-called Airy's stress function, and must satisfy the following constraint:

$$\Delta_{2D}^2 \Phi^{(i)} = -\frac{E_i H_i}{2} \mathcal{L}(w^{(i)}, w^{(i)}). \tag{4}$$

(1) and (4) must be considered, then, as a set of two coupled equations for each plate.

The second line of (1) includes the external forces acting on the plate. f_i^+ and f_i^- represent the pressure of air acting above and below the surface, while $f_{i,exc}$ is the excitation force. Their explicit expressions will be given below.

Appropriate conditions must be supplied at the boundary of $\mathcal{P}_i$ for both $w^{(i)}$ and $\Phi^{(i)}$. For $w^{(i)}$, there are three interesting options from a sound synthesis point of view: clamped, simply supported and free conditions. For $\Phi^{(i)}$, instead, the usual choice is free condition. (See [13] for details.)

2.2. Air

The air surrounding the plates is described by a velocity potential $\Psi(x, y, z, t)$ which satisfies the wave equation:

$$\partial_{tt}\Psi = c_a^2 \Delta_{3D}\Psi, \tag{5}$$

where c_a is the speed of sound in air (here, 340 m/s), and Δ_{3D} is the 3D Laplacian. Ψ is related to the more familiar quantities p and $\mathbf{v}$ (pressure and particle velocity) by:

$$p = \rho_a \partial_t \Psi \qquad \mathbf{v} = -\vec{\nabla}_{3D}\Psi, \tag{6}$$

where ρ_a is the density of air (1.21 kg/m^3) and $\vec{\nabla}_{3D}$ is the 3D gradient.

At the boundary $\partial\mathcal{V}$ of the computational box it is necessary to implement absorbing conditions. One possible choice, which is convenient for reducing the computational complexity of the scheme, is a first-order Engquist Majda condition [14], defined as:

$$\partial_t\Psi + c_a \mathbf{n} \cdot \vec{\nabla}_{3D}\Psi = 0, \tag{7}$$

where $\mathbf{n}$ denotes the unit vector normal to the wall and pointing outwards.

2.3. Coupling Conditions

Coupling conditions between the plate and the air can be obtained by enforcing continuity of pressure p and particle velocity v at the interface. When considering the acoustic field Ψ, they can be written as

$$f_i^+ = -\rho_a \lim_{z \to z_c^{i,+}} \partial_t \Psi\,|_{\mathcal{P}_i} \qquad f_i^- = \rho_a \lim_{z \to z_c^{i,-}} \partial_t \Psi\,|_{\mathcal{P}_i}, \tag{8}$$

and

$$\partial_t w_i = -\lim_{z \to z_c^{i,-}} \partial_z \Psi\,|_{\mathcal{P}_i} = -\lim_{z \to z_c^{i,+}} \partial_z \Psi\,|_{\mathcal{P}_i}. \tag{9}$$

These conditions hold over the plate regions $\mathcal{P}_i$.

3. FINITE DIFFERENCE IMPLEMENTATION

The numerical implementation of the model has been performed using finite difference time domain methods [15]. Possible schemes for the non-linear plate are given in [16], while in [17] the coupling between the air and thin structures (membranes, in this case) is discussed. Therefore, implementation details will be omitted in the present work; the notation used here is drawn from [18].

The physical variables $w^{(i)}$ and Ψ are approximated over regular Cartesian grids, with spacings h_i and h_a, respectively. The discrete time step is $k = 1/F_s$, with sample rate F_s chosen *a priori*.

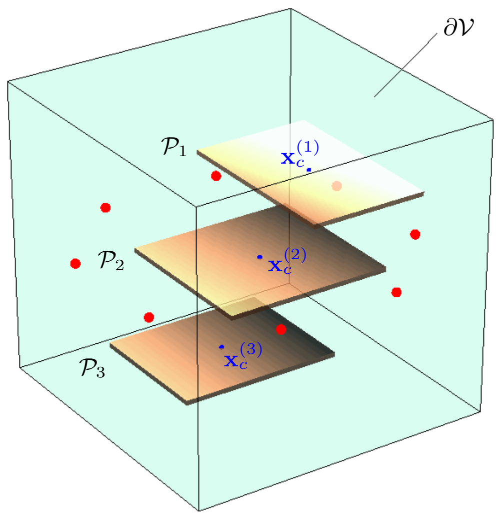

Figure 1: *Geometry of the model. Three plates $\mathcal{P}_1$, $\mathcal{P}_2$ and $\mathcal{P}_3$ are embedded within a 3D box $\mathcal{V}$. The boundary of the box is indicated with $\partial\mathcal{V}$. Centre positions for every plate are marked with their coordinates $\mathbf{x}_c^{(i)}$ (in blue). Possible output locations are marked with a ring of bold dots (in red).*

3.1. Scheme for the Plates

The displacement functions $w^{(i)}(x, y, t)$ for the various plates can be approximated as $w_{l,m}^{n,(i)}$, with $w_{l,m}^{n,(i)} \equiv w^{(i)}(lh, mh, nk)$ for integers l, m and n.

A discrete version of equations (1) and (4) for the i-th plate can be written as follows (retaining only the time index n):

$$\begin{aligned}\delta_{tt}w^n = &-\kappa^2\delta_{2\Delta}^2 w^n + \sigma\delta_{t-}\delta_{2\Delta}w^n + \frac{1}{\rho H}[(w^n, \mu_{t\cdot}\Phi^n) \\ &+ \frac{1}{\rho H}\left(f^+ + f^-\right) + \frac{1}{\rho H}\delta(l - l_0, m - m_0) f_{exc}\end{aligned} \tag{10}$$

$$\delta_{2\Delta}^2\left(\mu_{t+}\Phi^n\right) = -\frac{EH}{2}[(w^{n+1}, w^n), \tag{11}$$

where l_0 and m_0 are the coordinates of the nearest grid point to the continuous strike location. The various operators involved in the previous equations behave as following:

$$\delta_{tt}w_{l,m}^n = \frac{1}{k^2}\left(w_{l,m}^{n+1} + w_{l,m}^{n-1} - 2w_{l,m}^n\right), \tag{12a}$$

$$\delta_{2\Delta}w_{l,m}^n = \left(\delta_{xx} + \delta_{yy}\right)w_{l,m}^n \tag{12b}$$

$$\delta_{xx}w_{l,m}^n = \frac{1}{h^2}\left(w_{l+1,m}^n + w_{l-1,m}^n - 2w_{l,m}^n\right) \tag{12c}$$

$$\delta_{t-}w_{l,m}^n = \frac{1}{k}\left(w_{l,m}^n - w_{l,m}^{n-1}\right) \tag{12d}$$

$$\mu_{t\cdot}\Phi^n = \frac{1}{2}\left(\Phi^{n+1} + \Phi^{n-1}\right) \tag{12e}$$

$$\mu_{t+}\Phi^n = \frac{1}{2}\left(\Phi^{n+1} + \Phi^n\right) \tag{12f}$$

where δ_{yy} is analogous to δ_{xx} in (12c) with l and m exchanged.

The choice for the discretization of the non-linear term in (1) and (4) is discussed in detail in [16], where the explicit expression for the operator $\mathfrak{l}$ is given, together with a finite difference version of the boundary conditions.

Coupling conditions will be discretized in Section 3.3, while the discrete excitation will be discussed in Section 4.2.

3.2. Scheme for the Acoustic Field

The acoustic field $\Psi(x, y, z, t)$ can be approximated as $\Psi^n_{l,m,p}$. The finite difference version of (5) is:

$$\delta_{tt}\Psi = c_a^2 \delta_{3\Delta}\Psi, \tag{13}$$

where the 3D Laplacian $\delta_{3\Delta}$ is simply an extension of the 2D operator (12b). A possible implementation of absorbing conditions (7) over the boundary $\partial\mathcal{V}$ of the box can be found in [17].

3.3. Discrete Coupling Conditions

A detailed discussion of the coupling mechanism can be found in [17], therefore only a schematic outline will be given here. The discrete vertical coordinate $z_c^{(i)}$ of each plate is slightly modified to the nearest value $\bar{z}_c^{(i)}$ that lies half way between two neighbouring slices Ψ_i^+ and Ψ_i^- of the acoustic field. Let $p_i^+ = \bar{z}_c^{(i)} + h_a/2$ and $p_i^- = \bar{z}_c^{(i)} - h_a/2$ be the coordinates of such slices. Moreover, two interpolants $\mathcal{I}_i$ and $\mathcal{J}_i$ must be defined between the two grids [18]. With these positions, (8) and (9) become:

$$f_i^+ = -\rho_a \mathcal{I}_i \delta_{t\cdot}\Psi_i^+, \qquad f_i^- = \rho_a \mathcal{I}_i \delta_{t\cdot}\Psi_i^-, \tag{14}$$

and

$$\mathcal{J}_i \delta_{t\cdot} w^{(i)} = -\delta_{z-}\Psi_i^+ = -\delta_{z+}\Psi_i^-. \tag{15}$$

3.4. Stability conditions

Stability conditions for the above schemes can be easily obtained via energy analysis techniques (see [18].) For the plates' grids, one obtains:

$$h_i^2 \geq 4k\sigma_i + 4k\sqrt{\sigma_i^2 + \kappa_i^2}, \tag{16}$$

while, for the acoustic field,

$$h_a^2 \geq 3c_a^2 k^2. \tag{17}$$

4. INSTRUMENT DESIGN, CONTROL AND OUTPUT

While designing a sound synthesis environment, one has to consider the parameters that a musician or composer will need to specify in order to create and play his or her own instrument. It is obvious that the more parameters there are, the more cumbersome the implementation will be. Furthermore, it has been shown that some physical quantities have more importance than others from a perceptual point of view [19].

In the present case, the various parameters can be grouped into three classes: instrument design, control and output.

4.1. Instrument Design

At the beginning of the code, the user has to specify the geometric and physical description of the system. The former includes number, position and dimensions of the plates, together with the size of the computational box; the latter refers to all the constants appearing in (1), as well as to the boundary conditions for the various plates. In this second case, rather than exploring the entire space of physical parameters, it is useful to lump some of them under different "labels" (like `steel`, `copper`, etc.) according to perceptual considerations.

4.2. Control

Control parameters define how the virtual instrument is played. In order to reduce an already heavy computational load, a single strike is modeled as a raised cosine over time [17]. The external force f_{exc} in (1) corresponding to a strike of duration τ starting at $t = 0$ can be written as:

$$f_{exc}(t) = \begin{cases} \frac{F_{max}}{2}(1 - \cos(2\pi t/\tau)) & \text{for } 0 \leq t \leq \tau, \\ 0 & \text{else} \end{cases} \tag{18}$$

where F_{max} is the maximum value of f_{exc}. A finite difference implementation of (18) is straightforward. Starting from this basic element, it is possible to create a series of strikes that can emulate complex gestures; the main difficulty, especially when the number of strikes becomes large, is in specifying for each of them F_{max}, τ, the starting instant of excitation T_{exc} and the striking position $P_{exc} = (x_{exc}, y_{exc})$. One possibility for avoiding the declaration of all these quantities is to randomize them (within predefined limits).

This simplified approach to strike generation, though perhaps slightly primitive in that it lacks the ability to capture more subtle features of the mallet interaction, such as contact-recontact phenomena, has been successfully used in the past in connection to the modular environment described in [7] to create several musical works. That being said, a mallet-plate interaction model [9] would probably allow the composer/musician a more precise control over the instrument. An efficient and stable implementation of this non-linear contact force [20] with the simultaneous presence of the plate non-linearity is currently under study.

4.3. Output

As already mentioned, the entire acoustic field is modeled explicitly here. This allows the musician to draw outputs from any position within the box, by sampling air pressure variations generated by strikes on the plates. Multi-channel sounds are an interesting possibility, and they present virtually no additional computation cost, as output writing involves only a few multiplications and additions. In this case, one has to specify only the coordinates for each output location. As this is a time domain simulation, a moving output position can also be easily implemented.

5. RESULTS

5.1. Interaction through Air

In this model, acoustic pressure generated by a strike on a single plate will propagate within the box and excite the other plates, as well. Figure 2 shows the behaviour of the system after a raised cosine strike on the first plate. The delay between the strike and the excitation of the second and third plate is apparent.

5.2. Sound example

Sound examples obtained with this virtual instrument can be found in the author's website:

`http://www2.ph.ed.ac.uk/~s1164558`

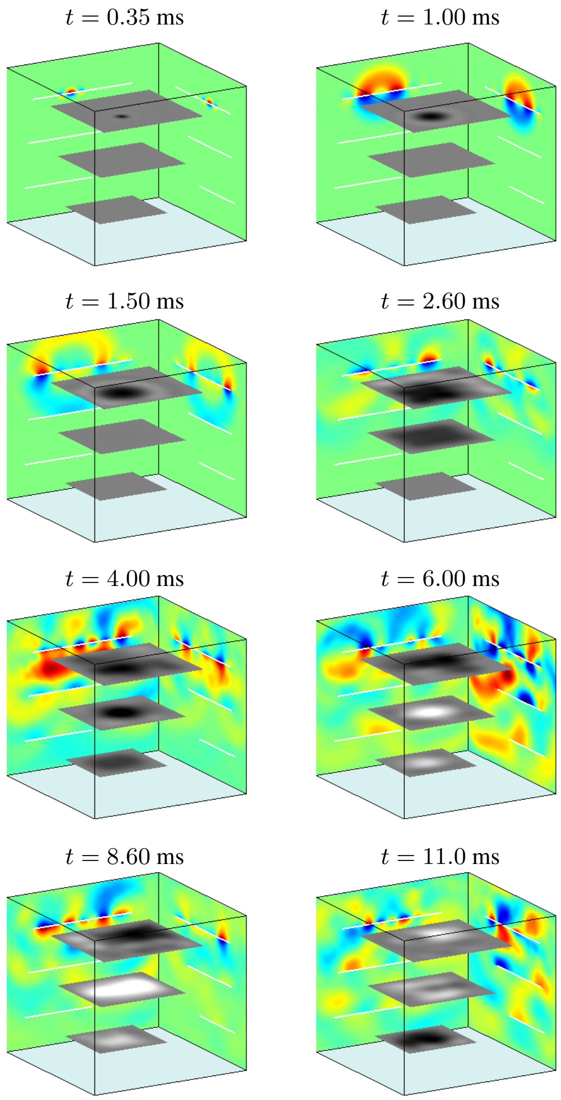

Figure 2: *Acoustic pressure propagation generated by a strike on the upper plate, at times as indicated. Central cross sections of the acoustic field along the xz and yz planes are plotted, as well. The projections of the plates on these planes are marked with white lines.*

6. CONCLUDING REMARKS

In this paper, a 3D environment based on a physical model of nonlinear plate vibration has been presented. It has been shown how a finite difference implementation of such a system offers enough flexibility to be used as a sound synthesis tool. Clearly, though, more work needs to be done in order to transform this into a mature musical instrument.

First of all, the usability of the system needs to be improved. On the one hand, it is necessary to define a "map" of perceptually meaningful physical parameters for the plates. This would spare the musician the daunting task of exploring a vast but sometimes perceptually redundant parameter space. On the other hand, the control strategy is still rather crude. When the number of strikes increases, the definition of hundreds of numbers could become a lengthy process. To this end, randomization of strikes offers some advantages, but may limit the creativity of the composer. A viable option could be the use of breakpoint functions over time to describe the global behaviour of relevant variables.

Secondly, many additional features could be added in order to obtain more interesting sounds. Some possibilities are spring-damper connections between the plates [7], bowing gestures [18], binaural sound output location [21]. By working with musicians and composers at Edinburgh University we look forward to exploring the strengths and the limits of the current model, and make improvements to it accordingly.

The computational complexity of this model has not been discussed in this paper. As is often the case for finite difference simulations, the algorithm presented above could require even several hours of computation in MATLAB for few seconds of output, depending on the number and sizes of the plates! This sometimes discouraging issue can be overcome with the use of parallel hardware, such as graphical processing units (GPGPUs). Possible speed-ups could be as far as tens of times [10, 22]. Algorithms for a fast parallel implementation of the present model are currently under study at Edinburgh University.

7. ACKNOWLEDGMENTS

Thanks to the anonymous reviewers for the useful comments and suggestions on how to improve this work.

8. REFERENCES

[1] A. Chaigne, C. Touzé, and O. Thomas, "Nonlinear vibrations and chaos in gongs and cymbals," *Acoustical science and technology*, vol. 26, no. 5, pp. 403–409, 2005.

[2] S. A. Van Duyne, *Digital Filter Applications to Modeling Wave Propagation in Springs, Strings, Membranes and Acoustical Space*, Ph.D. thesis, Center for Computer Research in Music and Acoustics, Stanford University, Stanford, CA, 2007.

[3] M. Ducceschi, C. Touzé, and S. Bilbao, "Nonlinear plate vibrations: A modal approach with application to cymbals and gongs," in *Proceedings of the Acoustics 2012 Nantes Conference*, Nantes, France, 2012.

[4] C. Cadoz, A. Luciani, and J. L. Florens, "CORDIS-ANIMA: a modeling and simulation system for sound and image synthesis: the general formalism," *Computer Music Journal*, vol. 17, no. 1, pp. 19–29, 1993.

[5] J. D. Morrison and J.-M. Adrien, "Mosaic: A framework for modal synthesis," *Computer Music Journal*, vol. 17, no. 1, pp. 45–56, 1993.

[6] G. Eckel, F. Iovino, and R. Caussé, "Sound synthesis by physical modelling with Modalys," in *Proc. International Symposium on Musical Acoustics*, Dourdan, France, 1995, pp. 479–482.

[7] S. Bilbao, "A modular percussion synthesis environment," in *Proc. of the 12th Int. Conference on Digital Audio Effects (DAFx-09)*, Como, Italy, 2009.

[8] F. Avanzini and R. Marogna, "A modular physically based approach to the sound synthesis of membrane percussion instruments," *Audio, Speech, and Language Processing, IEEE Transactions on*, vol. 18, no. 4, pp. 891–902, 2010.

[9] L. Rhaouti, A. Chaigne, and P. Joly, "Time-domain modeling and numerical simulation of a kettledrum," *The Journal of the Acoustical Society of America*, vol. 105, pp. 3545, 1999.

[10] S. Bilbao and C. J. Webb, "Timpani drum synthesis in 3D on GPGPUs," in *Proc. of the 15th Int. Conference on Digital Audio Effects (DAFx-12)*, York, United Kingdom, 2012.

[11] A. Chaigne and C. Lambourg, "Time-domain simulation of damped impacted plates. I. Theory and experiments," *The Journal of the Acoustical Society of America*, vol. 109, pp. 1422, 2001.

[12] A. Nayfeh and D. Mook, *Nonlinear oscillations*, John Wiley and Sons, New York, 1979.

[13] O. Thomas and S. Bilbao, "Geometrically nonlinear flexural vibrations of plates: In-plane boundary conditions and some symmetry properties," *Journal of Sound and Vibration*, vol. 315, no. 3, pp. 569–590, 2008.

[14] B. Engquist and A. Majda, "Absorbing boundary conditions for numerical simulation of waves," *Proceedings of the National Academy of Sciences*, vol. 74, no. 5, pp. 1765–1766, 1977.

[15] B. Gustafsson, H.-O. Kreiss, and J. Oliger, *Time dependent problems and difference methods*, Wiley New York, 1995.

[16] S. Bilbao, "A family of conservative finite difference schemes for the dynamical von Karman plate equations," *Numerical Methods for Partial Differential Equations*, vol. 24, no. 1, pp. 193–216, 2007.

[17] S. Bilbao, "Time domain simulation and sound synthesis for the snare drum," *The Journal of the Acoustical Society of America*, vol. 131, pp. 914, 2012.

[18] S. Bilbao, *Numerical Sound Synthesis: Finite Difference Schemes and Simulation in Musical Acoustics*, Wiley Publishing, Chichester, United Kingdom, 2009.

[19] M. Aramaki, C. Gondre, R. Kronland-Martinet, T. Voinier, S. Ystad, et al., "Thinking the sounds: An intuitive control of an impact sound synthesizer," in *Proceedings of the International Conference on Auditory Display*, Copenhagen, Denmark, 2009, pp. 119–124.

[20] F. Avanzini and D. Rocchesso, "Modeling collision sounds: Non-linear contact force," in *Proc. COST-G6 Conf. Digital Audio Effects (DAFx-01)*, Limerick, Ireland, 2001.

[21] C. J. Webb and S. Bilbao, "Binaural simulations using audio rate FDTD schemes and CUDA," in *Proc. of the 15th Int. Conference on Digital Audio Effects (DAFx-12)*, York, United Kingdom, 2012.

[22] L. Savioja, D. Manocha, and M. Lin, "Use of GPUs in room acoustic modeling and auralization," in *Proc. Int. Symposium on Room Acoustics*, Melbourne, Australia, 2010.